

Quasi-Stationary Waves in the Southern Hemisphere. Part I: Observational Data

ARTURO I. QUINTANAR AND CARLOS R. MECHOSO

Department of Atmospheric Sciences, University of California at Los Angeles, Los Angeles, California

(Manuscript received 18 August 1994, in final form 23 March 1995)

ABSTRACT

This Part I presents selected major features of the quasi-stationary (monthly mean) wave field in the troposphere and stratosphere of the Southern Hemisphere. It is confirmed that the quasi-stationary wave with zonal wavenumber 1 (QS-wave 1) is by far the dominant component of the geopotential height field at tropospheric and stratospheric levels. The amplitude of this wave is largest at about 60°S all year round and reaches a maximum during September and October in the upper troposphere and stratosphere.

Analysis of the Eliassen–Palm flux vector suggests that at high latitudes the quasi-stationary wave field is primarily forced from lower latitudes, most prominently from the Indian Ocean region during June and October. Orographic and thermal forcing from Antarctic regions seem to also be important sources of wave activity in polar and high latitudes, particularly over southern South America and the Atlantic Ocean.

The contribution to the quasi-stationary flow by the transient component of the flow is also analyzed. This analysis suggests that at high latitudes, the low-frequency transients act to strengthen QS-wave 1, while high-frequency transients weaken it. The values found for these contributions suggest that the low-frequency component is dominant.

1. Introduction

This is a two-part study of the quasi-stationary, planetary wave field in the Southern Hemisphere. In Part I, we present outstanding features of the field, with emphasis on the following aspects: 1) seasonal evolution, 2) propagation of planetary wave activity, and 3) forcing by transients. In Part II, we examine hypotheses on the generation mechanisms of the field.

Most previous studies of quasi-stationary waves in the Southern Hemisphere focused on the winter and summer seasons (e.g., van Loon and Jenne 1972; Hartmann 1977; Trenberth 1980; Karoly 1985). Randel (1988) examined other seasons and showed that the quasi-stationary wave variance in the southern troposphere has relative maxima at upper levels in the latitude bands 30°–40°S and 50°–60°S during late austral winter/early austral spring. The wave variance in the southern stratosphere has relative maxima in the latitude band 50°–60°S during the austral fall and spring seasons. The primary contribution to the quasi-stationary wave variance and corresponding poleward fluxes of momentum and heat in both the southern troposphere and stratosphere is provided by the component of the flow with zonal wavenumber 1. We will refer to this component of the quasi-stationary flow as QS-wave 1. Other planetary waves in the Southern Hemisphere

are primarily eastward moving (Mechoso and Hartmann 1982).

The existence of a prominent QS-wave 1 in the southern troposphere and stratosphere at high and polar latitudes (50°–70°S and 70°–90°S, respectively) has been linked to the zonal asymmetries in the Antarctic orography (e.g., James 1988) and in the strong subsidence associated with the efficient radiative cooling at the Antarctic surface (e.g., James 1989; Parish 1984). Our two-part study challenges this view for the high latitudes, where QS-wave 1 has the largest amplitudes. We will present evidence that strongly supports the hypothesis that QS-wave 1 in these latitudes is primarily forced by factors *other than* the Antarctic orography and associated thermal effects. We will also present evidence, however, that other planetary waves are significantly influenced by the zonal asymmetries of Antarctica and other geographic features of the southern polar region.

We follow a two-pronged approach for this investigation: 1) observational data is analyzed to characterize the quasi-stationary wave field and 2) a general circulation model (GCM) of the atmosphere is used to test hypotheses on the mechanisms at work for generation of the field. Part I concentrates on the first approach, and is organized as follows. Section 2 introduces the observational datasets selected for the study. Section 3 describes the seasonal variations of QS-wave 1 in the southern troposphere and stratosphere, with emphasis on the austral spring (October). Section 4 compares the contributions of QS-wave 1 and other planetary

Corresponding author address: Dr. Arturo I. Quintanar, Centro de Ciencias de la Atmosfera, Circuito Exterior, Ciudad Universitaria, C.P. 04510 Mexico D.E., Mexico.

waves to the total zonal variance during October. Section 5 examines the propagation of planetary wave activity in the southern troposphere. Section 6 estimates the effect of low- and high-frequency transients on the time-mean flow. A summary of the results obtained in Part I is presented in section 7. Part II will discuss the GCM experiments and analyze their results.

2. Data

For the troposphere, we use the U.S. National Meteorological Center (NMC) daily analyses of geopotential and temperature fields produced by the Global Data Assimilation System (GDAS) for the pressure levels 1000, 850, 700, 500, 400, 300, 250, 200, 150, and 100 mb (MacPherson et al. 1979). For the stratosphere, we use the daily analyses produced by the Climate Analysis Center section of the NMC for the pressure levels 70, 50, 30, 10, 5, 2, 1, and .4 mb. The data corresponds to the period January 1979 through December 1990. Randel (1988) compared the seasonal evolution of QS-wave 1 obtained by using the analyses compiled by NMC for the period 1979–1986 and by the World Meteorological Center at Melbourne, Australia, for the period 1979–1985. He found that despite the differences in periods, observing systems and methods of analysis, the results obtained for middle and high latitudes agree very well between the two datasets. This agreement increases our confidence in the results obtained in this investigation.

Concerning the notation used in the text, let $\Phi(\lambda, \phi, p)$ be any quasi-stationary (monthly mean) field, where λ is longitude, ϕ is latitude, and p is pressure. The zonally asymmetric component of Φ is defined as

$$\Phi^* = \Phi - [\Phi], \quad (1)$$

where the square brackets denote a zonal mean. The total zonal variance of Φ is given by

$$A_i^2 = (\Phi - [\Phi])^2. \quad (2)$$

We can write the zonal wavenumber k component of Φ as

$$\Phi_k = A_k(\phi, p) \cos[k\lambda + \alpha_k(\phi, p)], \quad (3)$$

where A_k and α_k are the amplitude and phase of the component, respectively. It is clear that

$$A_i^2 = \sum_{k=1}^K A_k^2(\phi, p). \quad (4)$$

In our case, $K = 36$ since we interpolate the NMC tropospheric and stratospheric analyses to a $5^\circ \times 2.5^\circ$ lat grid.

3. Seasonal variability of the quasi-stationary wave field

Figure 1 shows an ensemble average of the zonally asymmetric component of the geopotential height field

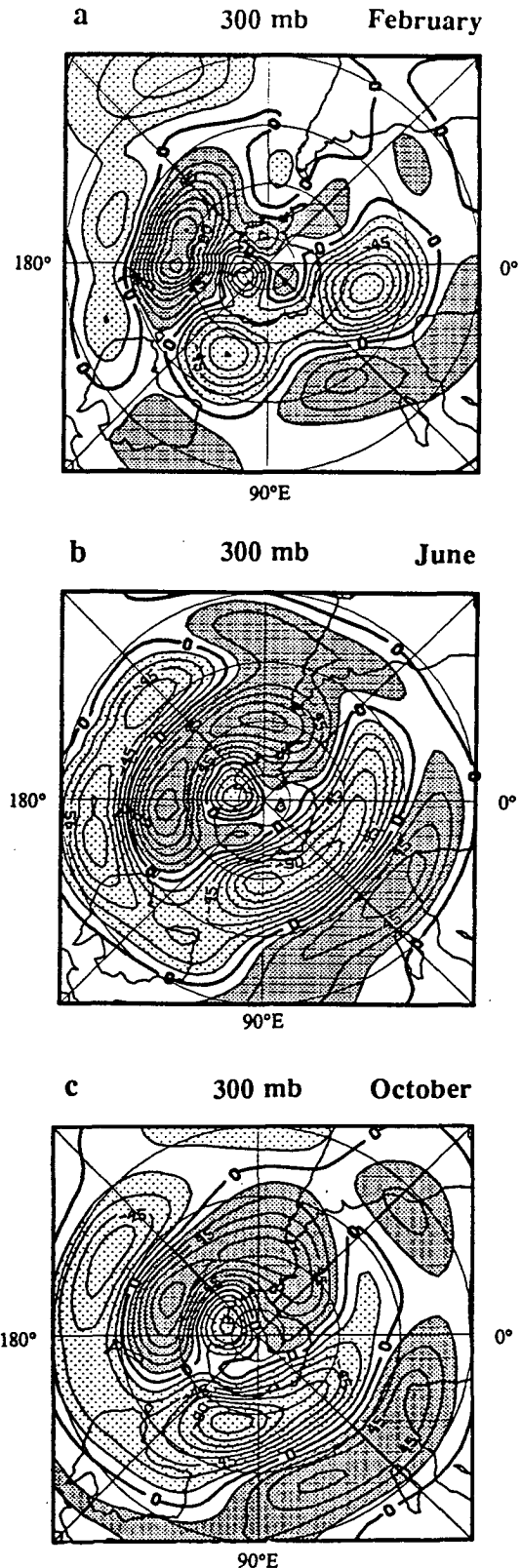


FIG. 1. The 300-mb zonal asymmetries of geopotential height for (a) February, (b) June, and (c) October. Dark and light shading corresponds to positive and negative values. The contour interval is 15 m.

at 300 mb for months in the austral summer (February), winter (June), and spring (October) during the 1979–90 period. The maps in Fig. 1 are very similar both in pattern and magnitude. In all cases, the largest amplitudes are at high latitudes (50° – 70° S), where the signature of QS-wave 1 is apparent. At these latitudes, the region of positive values extends roughly over the South Pacific Ocean, with largest amplitudes of about 100 m southeast of Australia. In both June and October, there are secondary maxima in the South American sector. The area of negative values is roughly over the south Atlantic and Indian Oceans, with largest magnitudes of about 120 m around 100° E. In February there is another area of strong negative values around 15° E. At polar latitudes (70° – 90° S) the positive (negative) values are roughly south of the negative (positive) values at high latitudes. There is a prominent low center over the Ross Sea, and positive values over the Weddell Sea and parts of East Antarctica. At midlatitudes (30° – 50° S) the pattern is in almost opposition of phase with that at high latitudes.

Figure 2 shows the zonally asymmetric component of the temperature field at 300 mb for February, June, and October. In general, the largest values are at polar latitudes, where the signature of QS-wave 1 is apparent. There are temperatures about 2° C colder than the zonal mean over East Antarctica, and warmer than the zonal mean over West Antarctica. At high and middle latitudes, contributions from smaller-scale waves to the temperature wave field are apparent.

Figure 3 shows maps of QS-wave 1 in the geopotential field at 300 mb for February, June, and October. For the months of June and October, the similarity between Figs. 1 and 3 is evidence of the dominant contribution of QS-wave 1 to the geopotential field in the southern troposphere. In February, QS-wave 1 contributes less. At high latitudes, the center of positive values is located in the South Pacific Ocean around 135° W. The wave amplitude increases about 40% from February to October. The wave phase, on the other hand, varies only slightly with time, as the pattern shown in Fig. 3 rotates slightly eastward. The wave phase at 300 mb tilts westward south of about 40° S, and eastward north of this latitude. A comparison between Figs. 1 and 3 shows that the center of negative values in the high latitudes at about 100° E is associated with waves shorter than QS-wave 1. In June and October, there are two less conspicuous centers of positive values at about 90° W and the date line, which are associated with QS-waves 2 and 3.

Figures 4 and 5 show longitude–height cross sections of QS-wave 1 in the geopotential height field at 55° and 75° S for February, June, and October. At 55° S in the stratosphere, the amplitude of QS-wave 1 increases systematically from February to October, when the largest values reach about 470 m at around 7 mb. At 75° S, QS-wave 1 in the stratosphere is slightly weaker than at 55° S. In the lower troposphere, there are

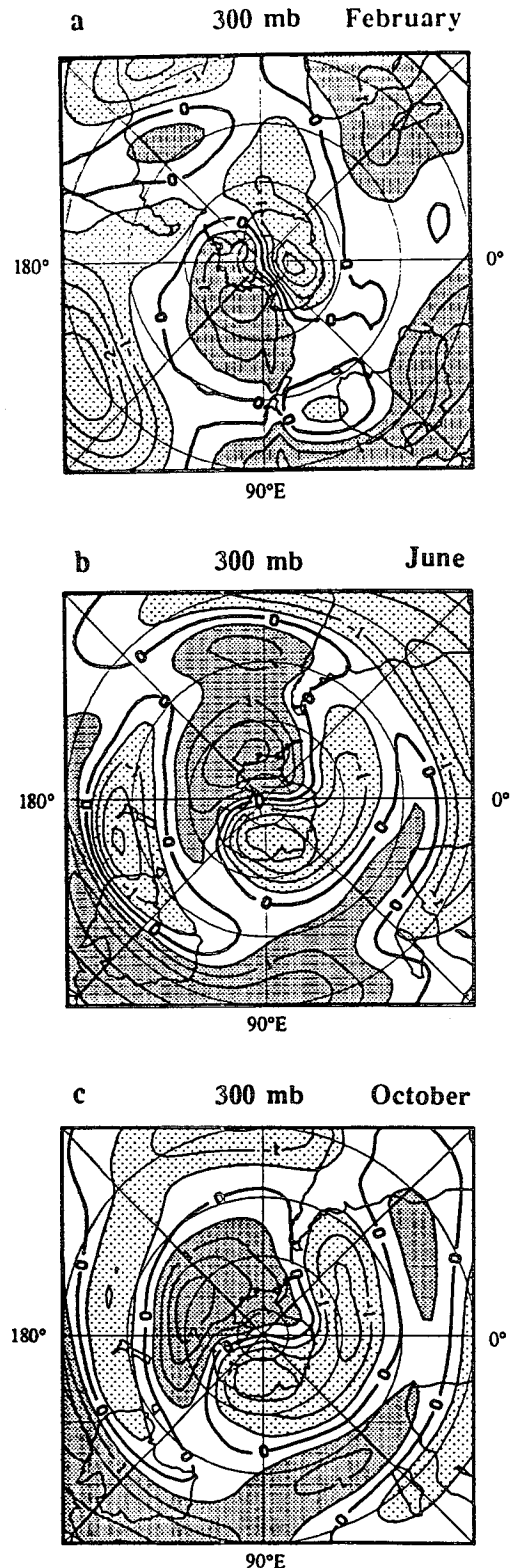


FIG. 2. As in Fig. 1 except for the temperature field. The contour interval is 0.5° C.

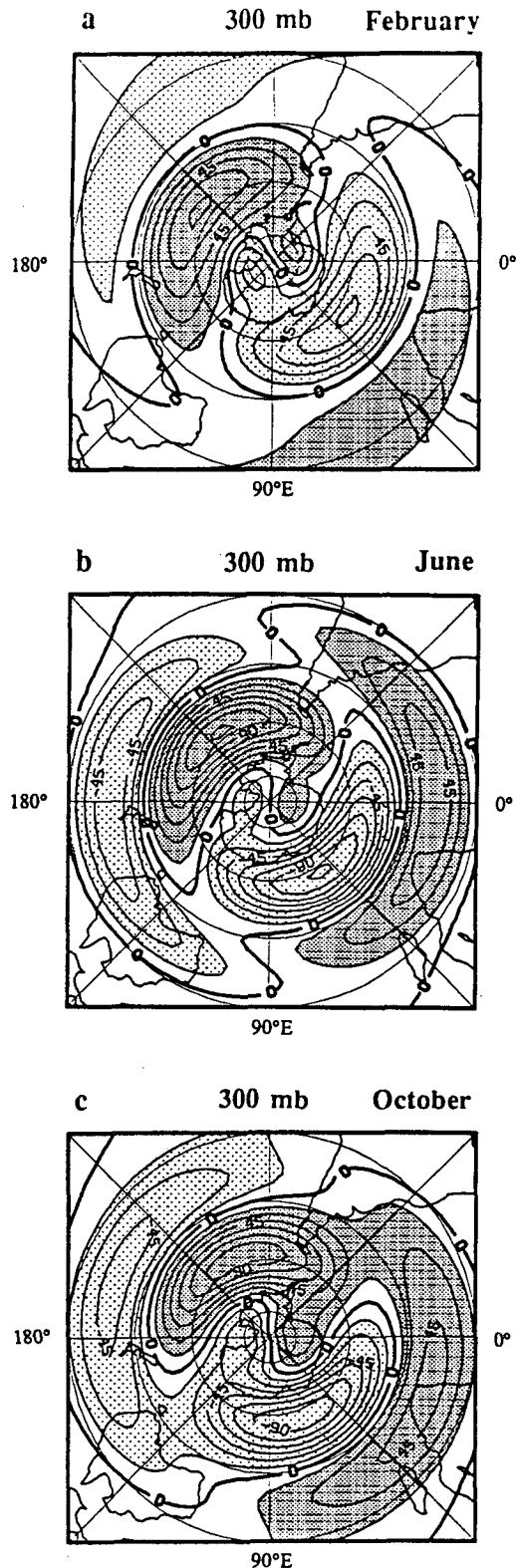


FIG. 3. The component with zonal wavenumber 1 of the fields shown in Fig. 1 (QS-wave 1). The contour interval is 15 m.

significant differences between Figs. 4 and 5 as QS-wave 1 at 55° and 75° are in opposition of phase. The structure of the geopotential height field in the lower troposphere reflects the semipermanent low-pressure center over the Ross Sea (e.g., Jenne et al. 1974), and high-pressure center over East Antarctica. The phase of QS-wave 1 tilts westward with height in the stratosphere. Consistent with this westward tilt and the increase in amplitude, the meridional heat transports associated with QS-wave 1 (not shown) also increase from February to October. These results are in general agreement with those reported by Randel (1988).

A comparison between Figs. 4 and 5 suggests that the Antarctic elevations induce anticyclonic vorticity on a shallow surface layer. (The vertical resolution of our dataset does not allow for an accurate estimate of the depth of this layer.) There is cyclonic vorticity above this layer. Such a vertical structure is expected as a consequence of a very efficient surface cooling, which results in strong drainage winds (katabatic winds). Katabatic winds blow toward the periphery of Antarctica inducing surface divergence that has to be balanced with convergence aloft. A meridional direct circulation is established by this mechanism (e.g., James 1989; Parish 1984). Recently, Juckes et al. (1994) have argued that this circulation is maintained through the action of synoptic-scale eddies that limit the strength of the polar vortex.

Figure 6 shows the seasonal variation of the amplitude of QS-wave 1 in geopotential height in the lower stratosphere (50 mb) and upper troposphere (300 mb). The values in Fig. 6 correspond to a 15-day running mean of the daily data. In the upper troposphere, the largest amplitudes of QS-wave 1 are in late austral winter–early spring (August and September) at high latitudes. There is also a weaker secondary peak in mid-latitudes during late austral winter. This behavior differs from that in the Northern Hemisphere (not shown), which shows a more pronounced seasonal cycle. In the lower stratosphere, the largest amplitudes are in the high latitudes with maxima in the austral winter and spring. Note the minimum in late austral winter, which does not have a clear counterpart in the troposphere.

The seasonal evolution of QS-wave 1 in the upper troposphere and stratosphere is qualitatively consistent with predictions of linear wave theory. The strong westerlies characteristic of the winter circulation are not suitable for vertical propagation of stationary wave activity from the troposphere into the stratosphere (Charney and Drazin 1961). The deceleration of the westerlies during spring as the final warming develops, therefore, is consistent with the strong planetary-scale disturbances that develop especially during the breakdown of the polar night vortex. Nevertheless, the evolution of the final stratospheric warming comprises both processes that are connected with others in the

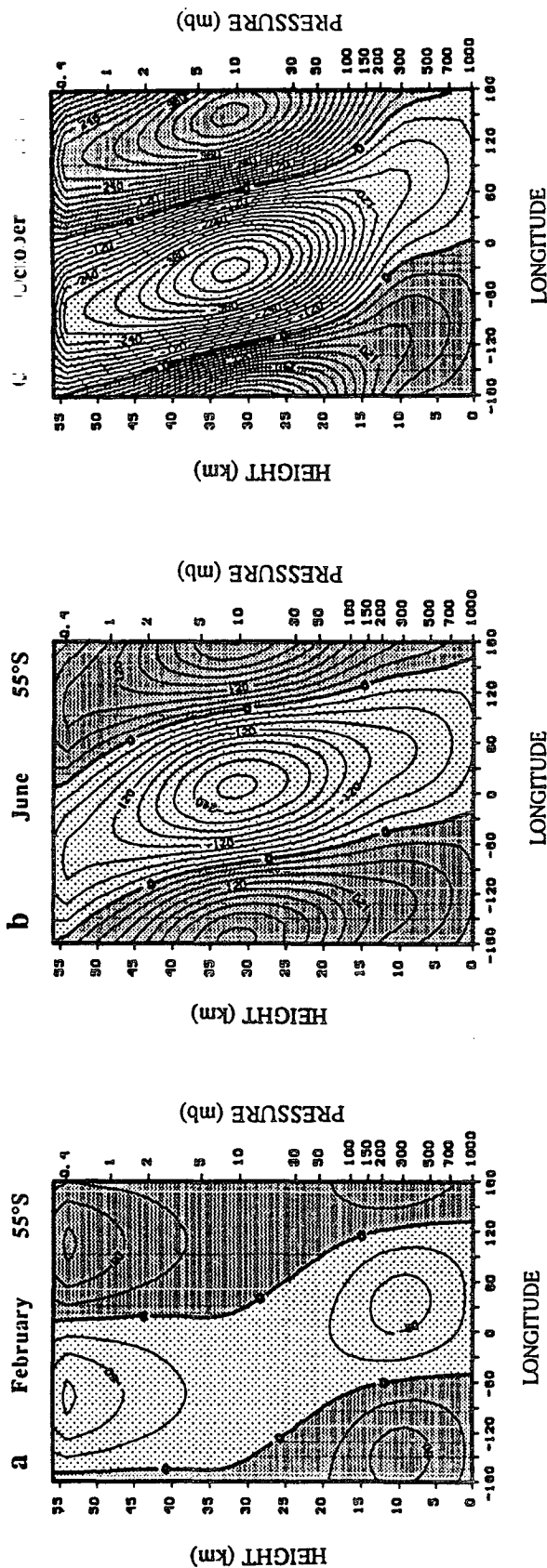


FIG. 4. Longitude-height diagrams at 55°S for the QS-wave 1 component of the geopotential height field for (a) February, (b) June, and (c) October. The contour interval is 30 m. Dark and light shading correspond to positive and negative values, respectively.

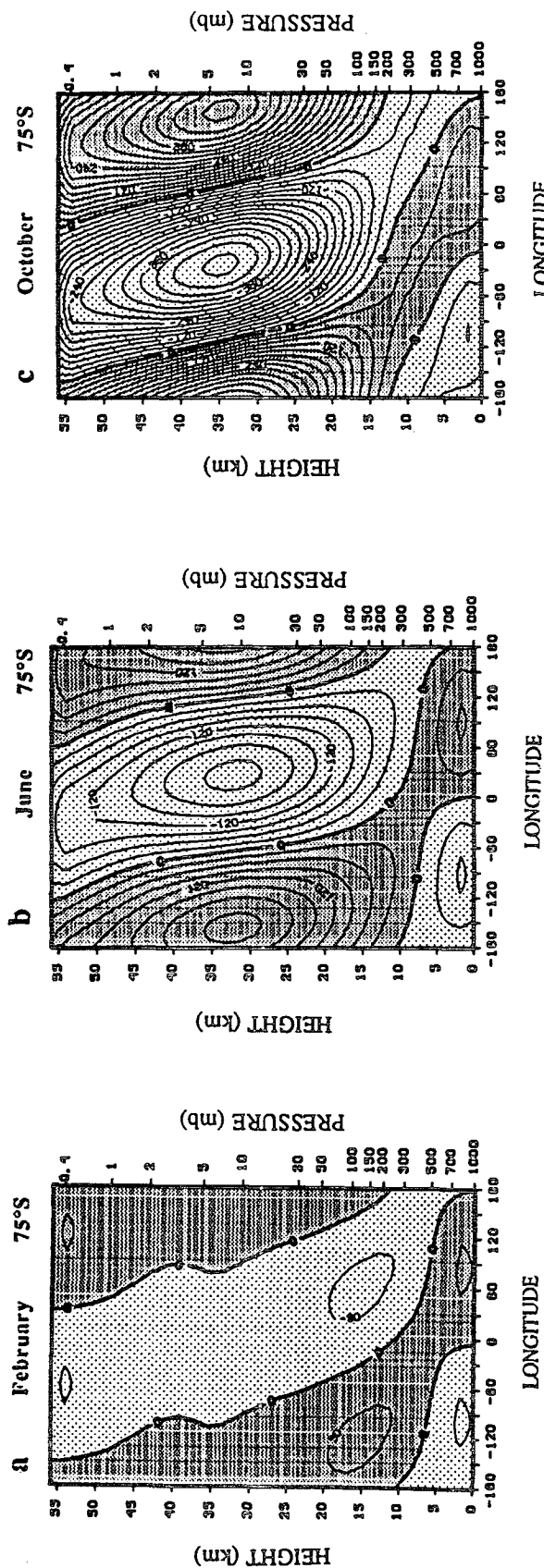


FIG. 5. As in Fig. 4 except at 75°S.

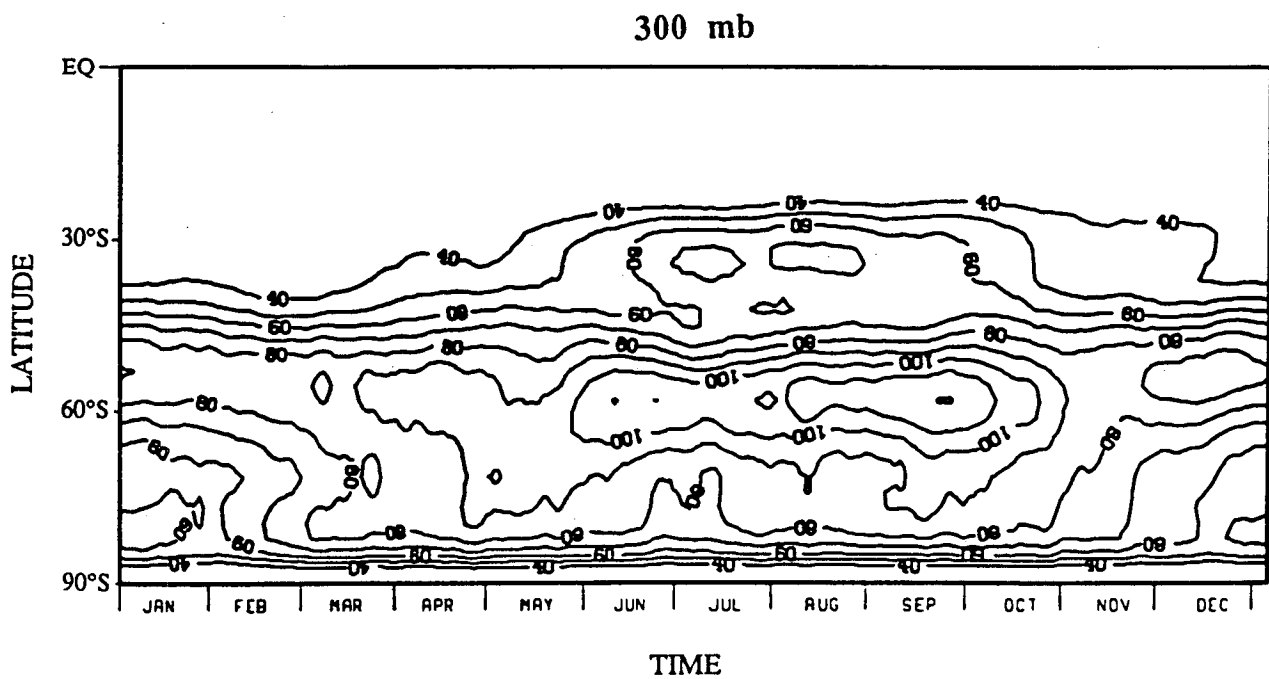
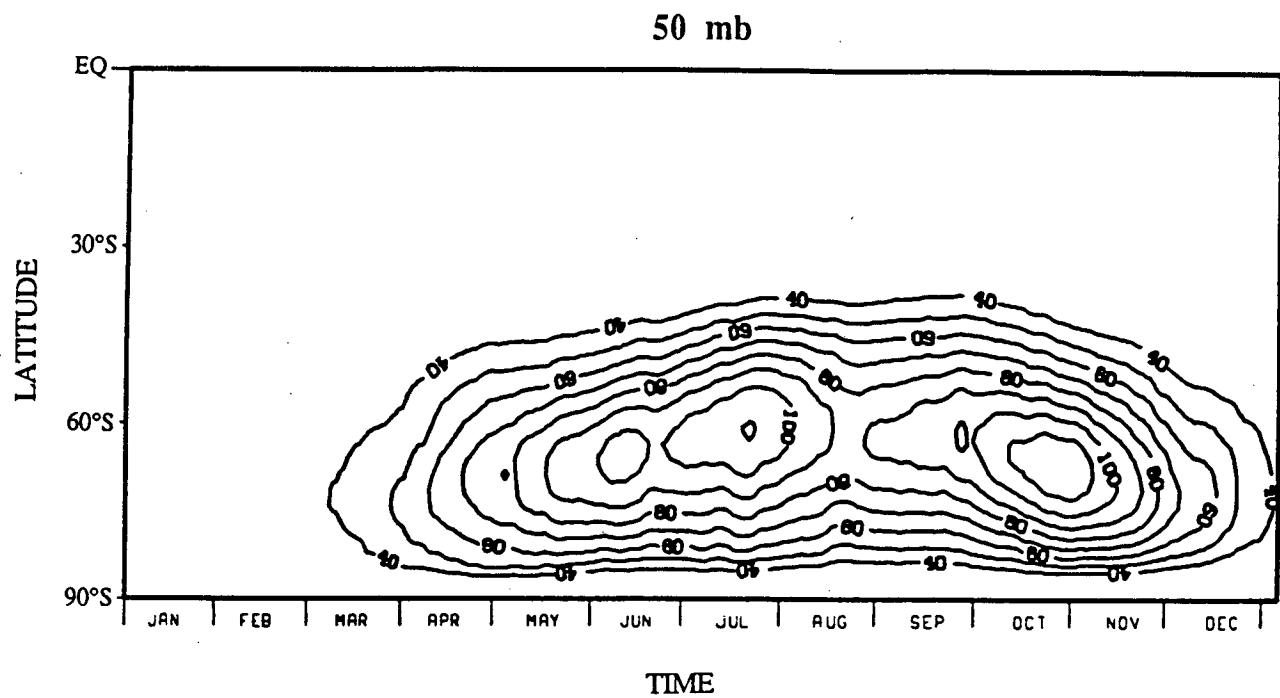


FIG. 6. Latitude-time diagrams of the seasonal evolution of the amplitude of wave 1 at 50 and 300 mb (contour interval 10 m).

troposphere, and others that primarily develop in situ (Mechoso et al. 1988; Mechoso 1990).

4. The zonal variance in October

Since the amplitude of QS-wave 1 is largest during October in the Southern Hemisphere, we concentrate on this period in this section. Figure 7 shows the total zonal variance in the October-mean geopotential height at 300 mb, the contributions to this variance of QS-waves 1, 2, and 3, and the range of values obtained for the period of analysis. In the Southern Hemisphere, the largest total variances are around 60°S, with hints of local maxima at about 35°S and 75°S. In the Northern Hemisphere there is a broad peak at about 55°N. The variability of the total variance is quite large, particularly in the high latitudes of the Northern Hemisphere. There are significant interhemispheric differences in the contributions of QS-waves 1, 2, and 3 to the total variance. At around 60°S and 45°N, QS-wave 1 contributes about 70% and 55% to the total zonal variance, respectively. In the Southern Hemisphere, the zonal variance for QS-wave 1 has a narrow bell-shaped distribution centered at high latitudes. In the Northern Hemisphere, the zonal variance of QS-wave 1 shows a more irregular structure over a wider latitudinal domain. In October, QS-wave 2 contributes about 10% to the total variance at 60°S, and about 55% at 60°N; QS-wave 3 contributes about 20% and 45% at those latitudes. Thus in October, QS-wave 1 is the main contributor to the Southern Hemisphere quasi-stationary wave field, and QS-waves 1 and 2 provide comparable contributions in the Northern Hemisphere.

5. Propagation of quasi-stationary planetary waves in the Southern Hemisphere

To study planetary wave propagation we inspect the distributions of the Eliassen–Palm (E–P) flux vector. Plumb (1985) derived a generalized expression for the E–P flux of wave activity for three-dimensional, stationary wave propagation. The expression for F derived by Plumb can be written as

$$F = (E_h, E_v), \tag{5}$$

where

$$E_h = \sigma \cos \phi \left[v^{*2} - \frac{1}{2a\Omega \sin 2\phi} \frac{\partial(v^*\Phi^*)}{\partial \lambda}, -u^*v^* + \frac{1}{2a\Omega \sin 2\phi} \frac{\partial(u^*\Phi^*)}{\partial \lambda} \right], \tag{6}$$

$$E_v = \sigma \cos \phi \left\{ \frac{\Omega \sin 2\phi}{S} \times \left[v^*T^* - \frac{1}{2a\Omega \sin 2\phi} \frac{\partial(T^*\Phi^*)}{\partial \lambda} \right] \right\}. \tag{7}$$

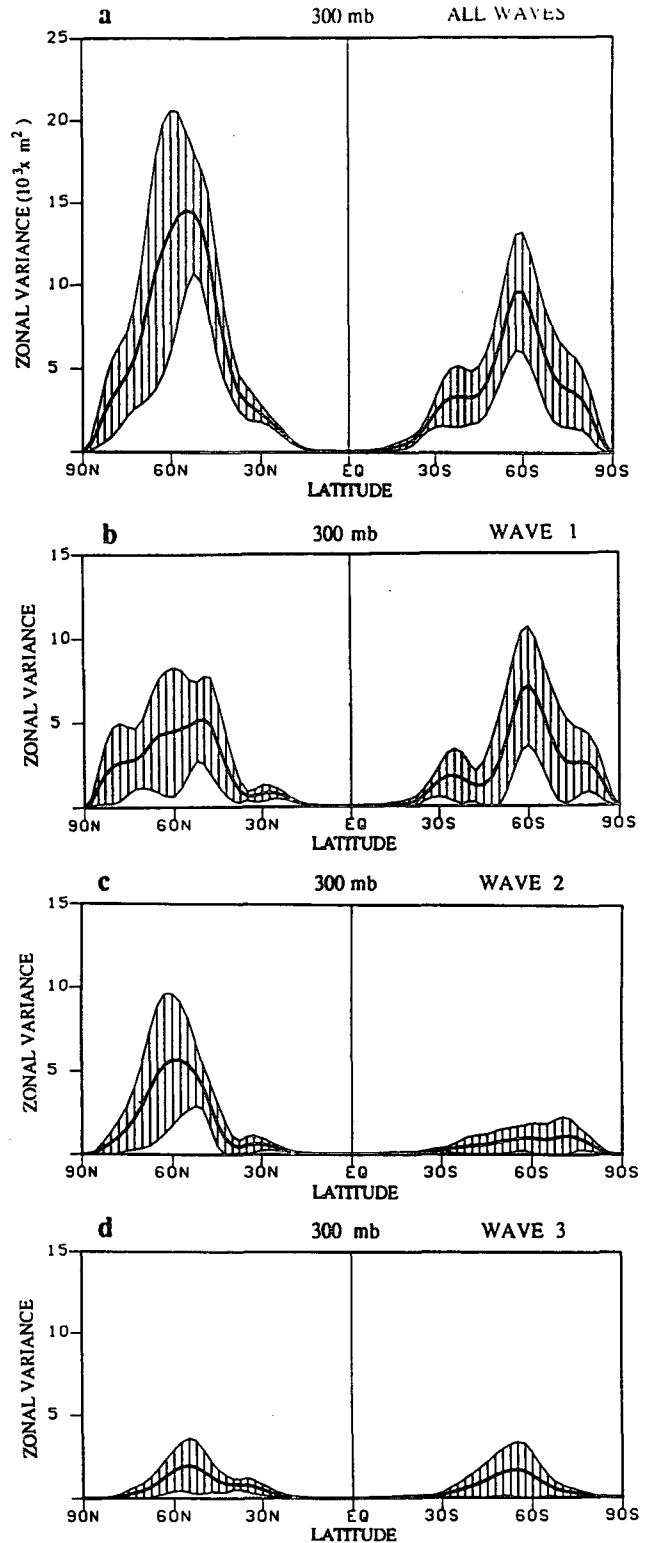


FIG. 7. Latitudinal distribution of the total zonal variance in the October-mean geopotential height field A^2 and contribution from QS-waves 1, 2, and 3 at 300 mb (thick solid line). The shaded region defines the interannual variation from the October monthly average.

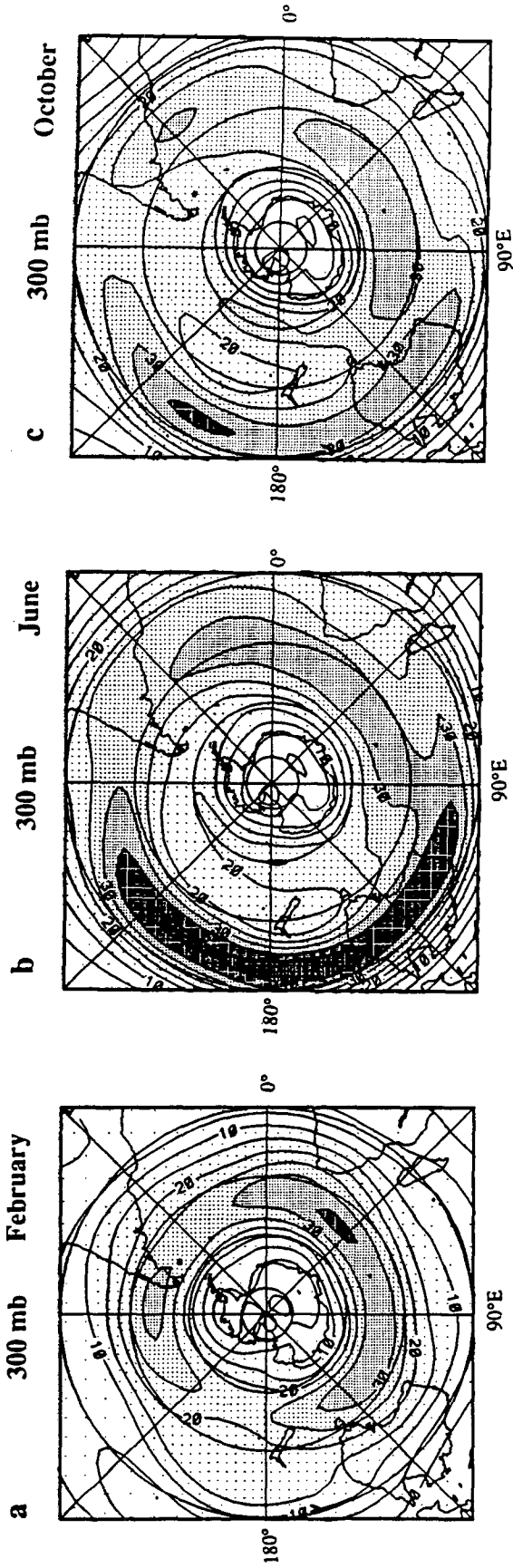


FIG. 8. The magnitude of the zonal components of the wind at 300 mb for (a) February, (b) June, and (c) October. The contour interval is 5 m s^{-1} .

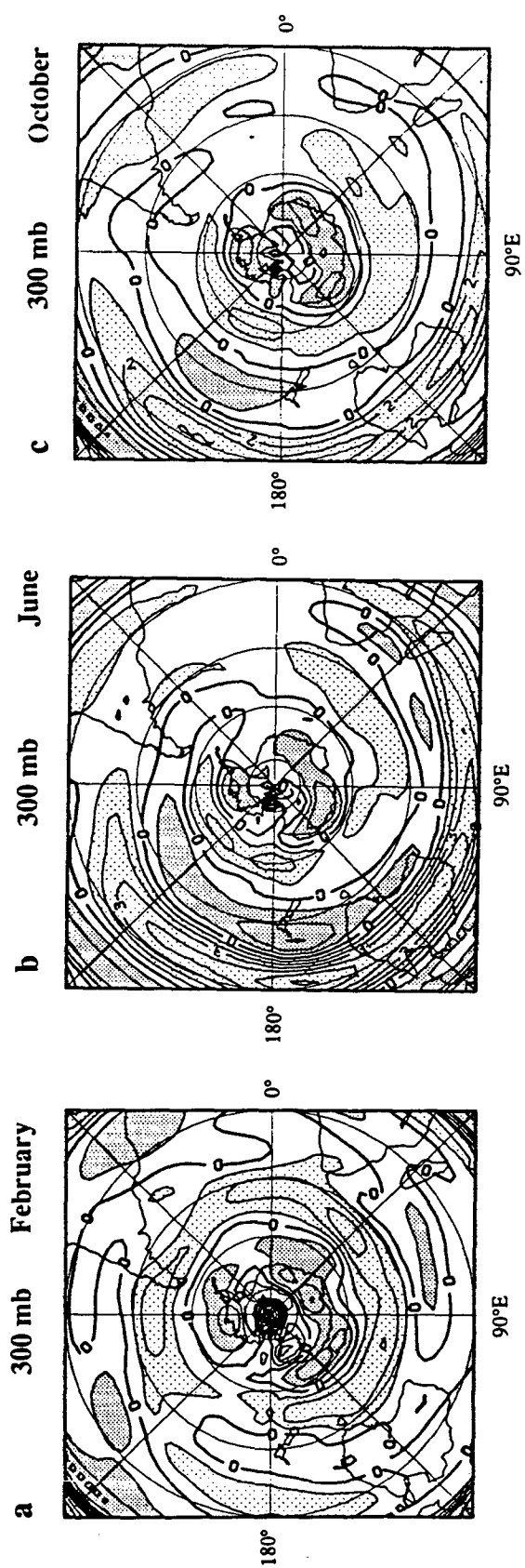


FIG. 9. As in Fig. 8 except for the meridional gradient of absolute vorticity. Heavier shading corresponds to values larger than $10^5 \text{ m}^{-1} \text{ s}^{-1}$, and the lighter shading to values smaller than $-10^5 \text{ m}^{-1} \text{ s}^{-1}$. The contour interval is $10^5 \text{ m}^{-1} \text{ s}^{-1}$.

Here, σ is the ratio between pressure and surface pressure; u and v are the zonal and meridional components of the horizontal wind, respectively; Φ is geopotential height; T is temperature; Ω and a are the angular velocity and radius of the earth, respectively; and S is the vertical temperature lapse rate (6.5 K km^{-1}). Here F can be interpreted as a measure of the net transfer rate of wave activity from one location to another (see Andrews and McIntyre 1976). Even in conservative flow, it can be shown that the vertical component of F , E_v , is zero only if the vertical velocity at the surface is zero (see Plumb 1985). Thus, topography is a source of stationary wave activity. The usefulness of the E–P flux diagnostics for analysis of quasi-stationary wave propagation is supported by the results obtained by using observational data (e.g., Plumb 1985; Karoly et al. 1989; Yang and Gutowski 1994); however, care must be exercised when interpreting the results of these diagnostics. Firstly, F was derived under a quasigeostrophic assumption and therefore its validity at low latitudes is suspect. Secondly, Plumb (1985) has shown that F is a nearly phase-independent quantity in the limit of almost-plane waves (i.e., the phase of the wave is a slowly varying function of space and time), and therefore we must be careful interpreting the short-scale quasi-stationary waves.

Before proceeding to inspect the E–P fluxes obtained for the Southern Hemisphere, we examine the distributions of the zonal component of the wind and meridional gradient of absolute vorticity. Divergent and convergent E–P fluxes in regions of westerly flow indicate sinks and sources of wave activity, respectively. Further, wave activity tends to be refracted toward regions where the meridional vorticity gradients are positive, and away from regions where it is negative (e.g., Hoskins and Karoly 1981; Webster and Holton 1982; Branstator 1983).

Figure 8 shows the zonal wind at 300 mb for February, June, and October. In February, there is a single jet at high latitudes from the southeast Pacific to south of Australia, with maximum wind speeds of about 30 m s^{-1} over South America and south of Africa. In June, a narrow subtropical jet centered at about 30°S extends from the Indian to the Pacific Ocean, with strongest winds from eastern Australia to the central Pacific. The jet at high latitudes extends from the Atlantic to the Pacific, so that a jet split is apparent over New Zealand. In the vertical, the jet core is between 300 and 200 mb (not shown). The zonal wind distribution in October is very similar to that in June, except that the jet split disappears in the lower stratosphere, where there is only a polar jet with speeds of about 45 m s^{-1} over the Madagascar sector (not shown).

Figure 9 shows that, in general, the meridional gradients of absolute vorticity are generally strongest near the strongest winds, and negative on the poleward side of the polar jet. In June and October, there are also negative meridional vorticity gradients on the poleward

and equatorward sides of the subtropical jet. According to the distributions shown in Fig. 9, the zonal wind during the austral winter and spring would act as a waveguide to focus the propagation of planetary wave activity in the Pacific and Indian Oceans from mid- to high latitudes. During February (i.e., the austral summer), the zonal wind distributions show weaker hemispheric asymmetries than during June and October, so that a different pattern of planetary wave propagation can be expected.

Figure 10 shows E_h and contours of E_v at 300 mb for February, June, and October. We start by discussing the results for E_v . In February, the distribution of E_v is not well organized, consisting primarily of small-scale features with weak magnitudes. In June, there are positive values of E_v over southern South America extending eastward, with largest values over the southwestern Atlantic at high latitudes and south of Australia. A pair of positive maxima is located at middle latitudes over the Western and Eastern Pacific. There are negative values in subtropical latitudes of the Eastern Hemisphere and at midlatitudes over the Pacific Ocean, as well as along the coast of East Antarctica. In October, E_v shows two prominent centers of positive values over southern South America and adjacent Atlantic Ocean and south of the Australian–New Zealand region. Negative values have generally small magnitudes at middle and subtropical latitudes over the Indian Ocean, the Western Pacific and over East Antarctica. Consistent with amplification of QS-wave 1 in the upper troposphere and stratosphere, we found significantly larger positive values for E_v at 100 mb (not shown). Also, the pattern of E_v is more zonally symmetric at higher levels, with maxima positioned again over the Australian–New Zealand region and over South America and the Atlantic Ocean.

Figure 11 shows that E_v at 500 mb for June and October has features not clearly seen at 300 mb. The largest positive values for E_v at 500 mb are over the Ross Sea and parts of Antarctica. A small region of negative values is over the periphery of East Antarctica. At high latitudes, there are positive values south of Australia. Another common feature to the maps for June and October is the tongue of positive values extending northeast from the Antarctic periphery toward southern South America. The distributions shown in Fig. 11 are in general agreement with those substantiated by Karoly (1985), who found that stationary waves in the winter and summer troposphere are not associated with sensible heat transports since they have an equivalent barotropic structure.

The distribution of E_h for February displayed in Fig. 10 is consistent with little or no propagation from the Tropics. The distributions of E_h for June and October in Fig. 10 show the signature of wave propagation from the Tropics along western and southern Australia. A comparison between Figs. 8 and 10 suggests that quasi-stationary wave activity in June and

October propagates preferentially along the waveguides defined by the zonal wind distribution. This wave propagation pattern is in agreement with results obtained during the austral winter by Karoly et al. (1989) and Yang and Gutowski (1994). From south of Australia, wave propagation continues poleward and eastward until either the waves are refracted equatorward over the central Pacific or continue propagating around Antarctica. The distributions of E_h corresponding to June and October in Figs. 10 and 11 also show propagation of wave activity northward and eastward from Antarctica into high latitudes over the Atlantic Ocean. This suggests that Antarctica is a source of wave activity not only at polar latitudes but also at high latitudes. The Antarctic orography and strong surface cooling are obvious candidates for this source of wave activity.

The significance of small-scale features over polar regions may come into question, since the contribution to the divergence of F by E_v is usually smaller than that of E_h , particularly during February. During June and October the contributions are of similar magnitude. Despite this problem we found the distributions of E_v to be vertically coherent in June and October.

In summary, the observational evidence suggests that propagation from both lower and polar latitudes contributes to the existence of QS-wave 1 in the high latitudes of the Southern Hemisphere. In this respect, the most important feature is propagation of wave activity from the tropical Indian Ocean into the high latitudes of the Pacific Ocean.

6. Effects of large-scale transient eddies on the mean flow

Transient eddies can also force quasi-stationary features of the flow. To explore this issue, we use the following equation (Holopainen 1978; Holopainen et al. 1982) for the time change of the quasi-stationary geopotential height ($\bar{\Phi}$) field,

$$\frac{\partial \bar{\Phi}}{\partial t} = -\frac{f}{g} \nabla^{-2} [\bar{v} \cdot \nabla (\bar{\zeta} + f)] + \frac{f}{g} \nabla^{-2} (k \cdot \nabla \times A_h), \quad (8)$$

where t is time, f is the Coriolis parameter, g is gravity, $\zeta = (g/f) \nabla^2 \bar{\Phi}$, overbars indicate monthly average. In addition,

$$A_h = A_\lambda i + A_\phi j, \quad (9)$$

$$A_\lambda = -\frac{1}{a \cos \phi} \frac{\partial \overline{u'u'}}{\partial \lambda} - \frac{1}{a \cos \phi} \frac{\partial \overline{u'v' \cos \phi}}{\partial \lambda} + \frac{\overline{u'v'}}{a} \tan \phi, \quad (10)$$

$$A_\phi = -\frac{1}{a \cos \phi} \frac{\partial \overline{u'v'}}{\partial \lambda} - \frac{1}{a \cos \phi} \frac{\partial \overline{v'v' \cos \phi}}{\partial \lambda} + \frac{\overline{u'u'}}{a} \tan \phi, \quad (11)$$

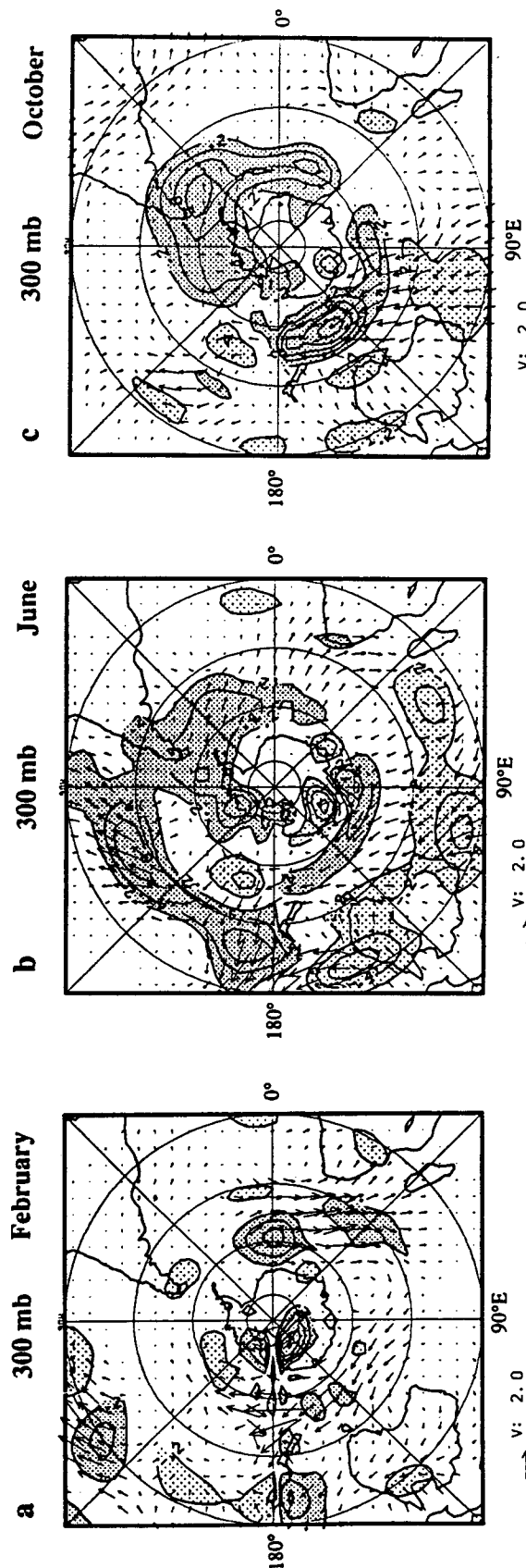


FIG. 10. The Eliassen-Palm flux of wave activity flux (F) at 300 mb for (a) February, (b) June, and (c) October. The arrows represent the horizontal component of F (E_h) and the contours represent the vertical component of F (E_v). The reference arrow is $2 \text{ m}^2 \text{ s}^{-2}$, and the contour interval is $10^{-2} \text{ m}^2 \text{ s}^{-2}$.

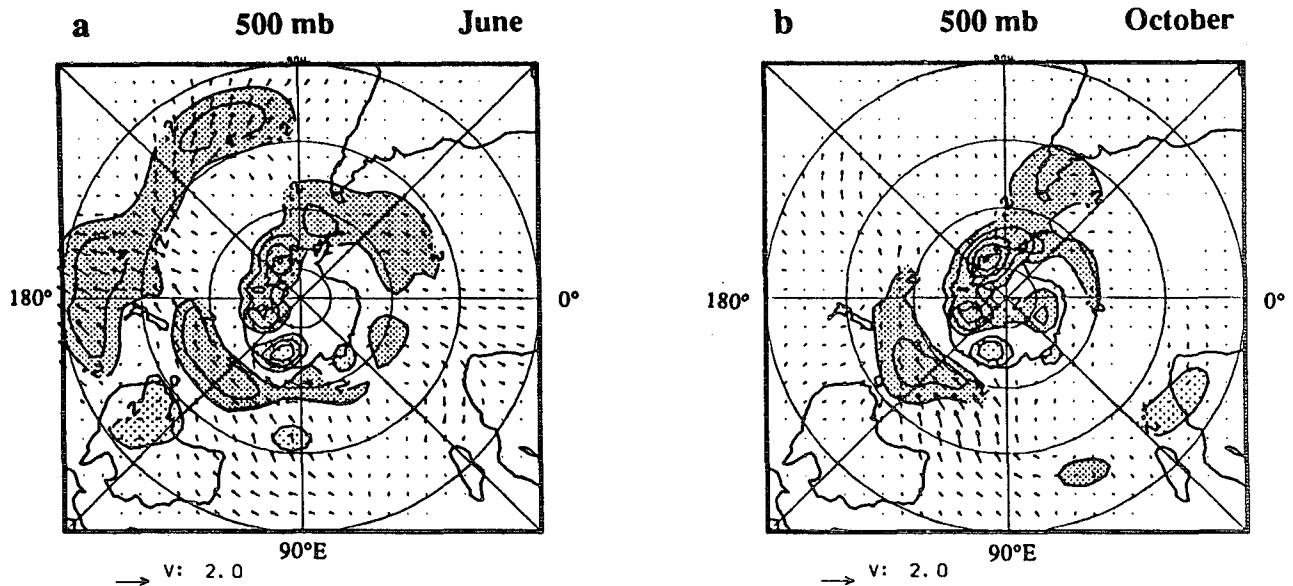


FIG. 11. As in Fig. 10 except for June and October at 500 mb.

where primes indicate fluctuations (i.e., the transient eddies), from the 12-yr mean (1979–1990). The high- and low-frequency transients of the flow are defined by applying a low-pass filter with a 15-day cutoff frequency to the resulting time series (see Blackmon 1976 for details about the filter). Transient eddy statistics are computed for each individual October and an ensemble average of these monthly statistics is then taken. The second term on the right-hand side of (8) represents the contribution to the time rate of change of the quasi-stationary geopotential height field by the transient eddies.

We start by presenting plots of the kinetic energy of the transient eddies, as well as that of the low- and high-pass transients (see Fig. 12). The kinetic energy of the transient eddies is largest at middle latitudes in a broad latitude belt that extends from the Pacific to the Indian Ocean, with maxima that approximately correspond to the location of subtropical and polar jet cores (see Fig. 8). This distribution is similar to that of the low-pass transients. The kinetic energy for the high-pass transients has comparable values, particularly over the Pacific and Indian Oceans and southeast of South America.

Figure 13 shows the zonally asymmetric component of the contribution to the time change of the quasi-stationary geopotential height field by transient eddies, as well as the contributions by the low- and high-pass transients. The contribution by transient eddies at middle, high, and polar latitudes has a zonal wavenumber 1 pattern, which resembles that of QS-wave 1 at high latitudes (see Fig. 2). The contribution by the low-pass transients has an even stronger resemblance with QS-wave 1. The contribution by the high-pass transients, on the other hand, primarily consists of small-scale structures and its zonal wavenumber 1 component is

almost 180° out of phase with QS-wave 1 at high latitudes. At polar latitudes, all contributions are almost in quadrature of phase with QS-wave 1. These results suggest that, at high latitudes, the low-pass transient eddies act to strengthen QS-wave 1, and that the high-pass transient eddies act to weaken it.

7. Summary and conclusions

Part I of this two-part study presents an observational characterization of the quasi-stationary wave field in the Southern Hemisphere troposphere and stratosphere. We used a 12-year long record (1979–90) of observational data prepared by the National Meteorological Center. We confirmed that the quasi-stationary wave with zonal wavenumber 1 (QS-wave 1) is by far the dominant component of the geopotential height field in the troposphere and stratosphere of the Southern Hemisphere, and concentrated on this feature of the flow.

The amplitude of QS-wave 1 is largest at high latitudes (50° – 70° S) all year round. The wave amplitude is approximately constant in time, except for a period of intense growth during the austral spring, particularly in the upper troposphere and stratosphere. The waves with zonal wavenumbers 2 and 3 contribute less to the quasi-stationary wave field, as they are primarily eastward traveling.

One of the principal results of this analysis is that remote forcing seems to play a key role in the generation and maintenance of QS-wave 1 at the high southern latitudes during the austral winter and spring. Our results of E–P flux computations show a prominent southward wave propagation from the Indian Ocean at subtropical latitudes. At high latitudes

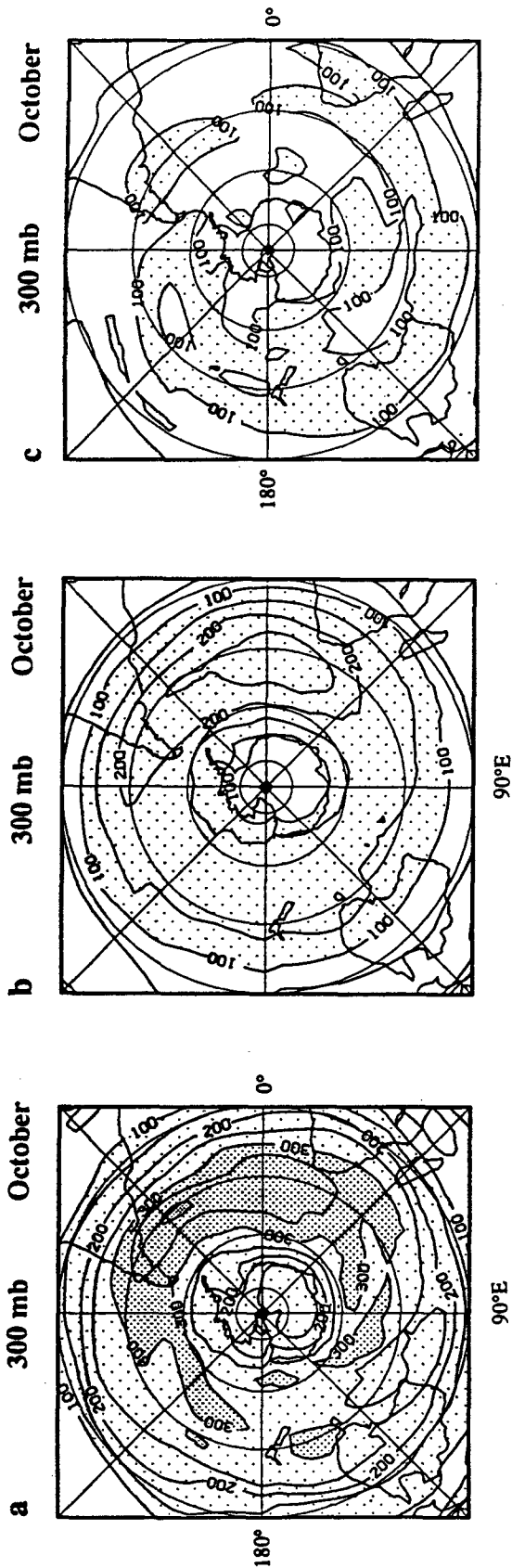


FIG. 12. Kinetic energy for October at 300 mb for (a) transient eddies and contributions by the low and high frequency transients (b) and (c), respectively. The contour interval is $50 \text{ m}^2 \text{ s}^{-2}$.

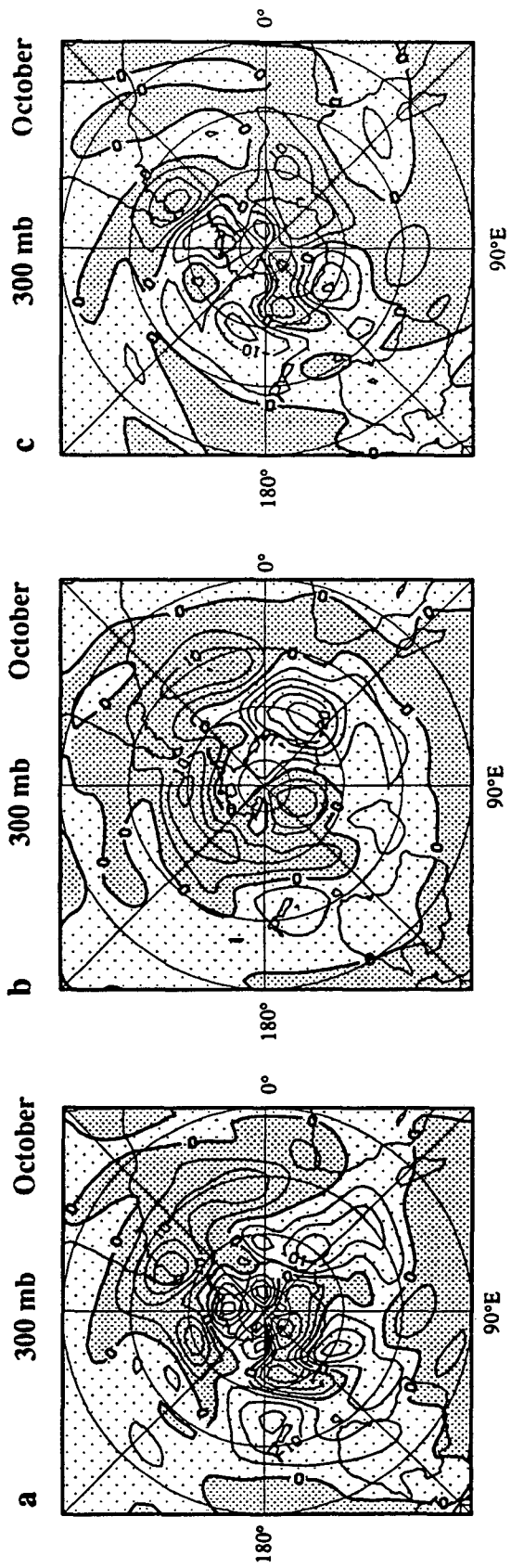


FIG. 13. Zonally asymmetric part of the contribution to the time change of the quasi-stationary component of the mean geopotential height field for October at 300 mb by (a) transient eddies, (b) low-pass transients, and (c) high-pass transients. The contour interval is 5 m day^{-1} . Dark and light shading correspond to positive and negative values, respectively.

south of Australia the wavetrain is refracted northward over the central Pacific Ocean. This behavior is consistent with previous studies of propagation of Rossby waves on the sphere forced by low-latitude diabatic heating (e.g., Hoskins and Karoly 1981; Hendon and Hartmann 1982), in which stationary waves with long wavelengths propagate strongly poleward and eastward.

Studies of Rossby waves propagating meridionally in a zonally homogeneous flow (e.g., Held 1983) show that the amplitude of stationary waves must increase as the wavetrain approaches a turning point. This can be qualitatively understood by recalling that the E–P flux is proportional to the product of meridional group velocity and the wave activity density (which in turn is proportional to the square of the wave amplitude) and is constant along a wavetrain. Thus the wave amplitude is expected to increase as the wavetrain approaches a turning point where the meridional group velocity is small. At high latitudes the Indian Ocean wavetrain reaches its turning point, which coincides with the latitudes where the amplitude of QS-wave 1 is largest.

In October at tropospheric levels, consistent with large meridional heat transports, vertical propagation of wave activity is largest at high latitudes. In contrast, in June, vertical propagation is weaker since waves in this time of the year exhibit a more barotropic vertical structure than in October and are thus associated with smaller meridional heat transports. During June and October wave activity also propagates horizontally and vertically from polar latitudes into high and middle latitudes over South America and the Atlantic Ocean.

The distribution of the vertical component of the E–P flux for October at various levels in the southern troposphere suggests that a fraction of the vertically propagating wave activity can be traced to the lower troposphere over the Antarctic region. Another source of vertically propagating wave activity is located south of Australia at about 60°S. We also analyzed the contributions of the quasi-stationary component of the flow by the low- and high-pass transients. The largest contributions by low-pass transients (periods longer than 15 days) were found in high latitudes, where QS-wave 1 has largest amplitudes. At these latitudes, the contribution is dominated by its component with zonal wavenumber 1, which is almost in phase with QS-wave 1. The contribution by high-pass transients (periods shorter than 15 days), on the other hand, is less dominated by its component with zonal wavenumber 1, which is in almost opposition of phase with QS-wave 1. The low-pass transients, therefore, act to strengthen QS-wave 1, whereas the high-pass transients weaken it. Since the magnitude of the former contribution is far stronger than that of the latter, these results suggest that the net effect of the transients is to enhance QS-wave 1. At polar latitudes, both the low- and high-frequency transients act to weaken the quasi-stationary wave field.

Acknowledgments. We are grateful to A. Arakawa for useful comments and to R. Lindzen for stimulating discussions. Ms. C. Wong and Ms. K. Hartman typed the manuscript. This research was supported by NSF ATM-8814892 and ATM-9122153, and by CalSpace under Grant CS-25-88.

REFERENCES

- Andrews, D. G., and McIntyre, 1976: Planetary waves in horizontal and vertical shear: The generalized Eliassen–Palm relation and the mean zonal acceleration. *J. Atmos. Sci.*, **33**, 2031–2048.
- Blackmon, M. L., 1976: A climatological spectral study of the 500 mb geopotential height of the Northern Hemisphere. *J. Atmos. Sci.*, **33**, 1607–1623.
- Branstator, G., 1983: Horizontal energy propagation in a barotropic atmosphere with meridional and zonal structure. *J. Atmos. Sci.*, **40**, 1689–1708.
- Charney, J. G., and P. G. Drazin, 1961: Propagation of planetary-scale disturbances from the lower into the upper atmosphere. *J. Geophys. Res.*, **66**, 83–109.
- Hartmann, D. L., 1977: Stationary planetary waves in the Southern Hemisphere. *J. Geophys. Res.*, **82**, 4930–4934.
- Held, I. M., 1983: Stationary and quasi-stationary eddies in the extratropical troposphere: Theory. *Large-scale Dynamical Processes in the Atmosphere*, B. J. Hoskins and R. P. Pearce, Eds., Academic Press, 127–168.
- Hendon, H. H., and D. L. Hartmann, 1982: Stationary waves on a sphere: Sensitivity to thermal forcing. *J. Atmos. Sci.*, **39**, 1906–1920.
- Holopainen, E. O., 1978: On the dynamic forcing of the long-term flow by the large-scale Reynolds' stresses in the atmosphere. *J. Atmos. Sci.*, **35**, 1596–1604.
- , L. Rontu, and N-C Lau, 1982: The effect of large-scale transient eddies on the time-mean flow in the atmosphere. *J. Atmos. Sci.*, **39**, 1972–1984.
- Hoskins, B. J., and D. J. Karoly, 1981: The steady linear response of a spherical atmosphere to thermal and orographic forcing. *J. Atmos. Sci.*, **38**, 1179–1196.
- James, I. N., 1988: On the forcing of planetary-scale Rossby waves by Antarctica. *Quart. J. Roy. Meteor. Soc.*, **114**, 619–637.
- , 1989: Antarctic drainage flow: Implications for hemispheric flow on the Southern Hemisphere. *Antarc. Sci.*, **1**, 279–290.
- Jenne, R. L., H. L. Crotcher, H. van Loon, and J. S. Taljaard, 1974: A selected climatology of the Southern Hemisphere: Computer methods and data availability. NCAR-TN STR 92. NCAR, Boulder, CO, 91 pp.
- Jukes, M. M., I. N. James, and M. Blackburn, 1994: The influence of Antarctica on the momentum budget of the southern extratropics. *Quart. J. Roy. Meteor. Soc.*, **120**, 1017–1044.
- Karoly, D. J., 1985: An atmospheric climatology of the Southern Hemisphere based on ten years of daily numerical analyses (1972–82). Part II: Standing wave climatology. *Aust. Meteor. Mag.*, **33**, 105–116.
- , R. A. Plumb, and M. Ting, 1989: Examples of horizontal propagation of quasi-stationary waves. *J. Atmos. Sci.*, **46**, 2802–2811.
- McPherson, R. D., K. H. Bergman, R. E. Kistler, G. E. Rasch, and D. S. Gordon, 1979: The NMC operational global data assimilation system. *Mon. Wea. Rev.*, **107**, 1445–1461.
- Mechoso, C. R., 1990: The final warming of the stratosphere. *Dynamics, Transport and Photochemistry of the Middle Atmosphere of the Southern Hemisphere*, A. O'Neill, Ed., Kluwer Academic Publishers, 55–69.
- , and D. L. Hartmann, 1982: An observational study of traveling planetary waves in the Southern Hemisphere. *J. Atmos. Sci.*, **39**, 1921–1935.

- , A. O'Neill, V. D. Pope, and J. D. Farrara, 1988: A study of the stratospheric final warming of 1982 in the Southern Hemisphere. *Quart. J. Roy. Meteor. Soc.*, **114**, 1365–1384.
- Parish, T., 1984: A numerical study of strong katabatic winds over Antarctica. *Mon. Wea. Rev.*, **112**, 545–554.
- Plumb, R. A., 1985: On the three-dimensional propagation of stationary waves. *J. Atmos. Sci.*, **42**, 217–229.
- Randel, W. J., 1988: The seasonal evolution of planetary waves in the Southern Hemisphere stratosphere and troposphere. *Quart. J. Roy. Meteor. Soc.*, **14**, 1385–1409.
- Trenberth, K. E., 1980: Planetary waves at 500 mb in the Southern Hemisphere. *Mon. Wea. Rev.*, **108**, 1378–1389.
- van Loon, H., and R. L. Jenne, 1972: The zonal harmonic standing waves in the Southern Hemisphere. *J. Geophys. Res.*, **77**, 992–1003.
- Webster, P. J., and J. R. Holton, 1982: Cross equatorial response to middle latitude forcing in a zonally varying basic state. *J. Atmos. Sci.*, **39**, 722–733.
- Yang, S., and W. J. Gutowski, Jr., 1994: GCM Simulations of the three-dimensional propagation of stationary waves. *J. Climate*, **7**, 414–432.